Eur. Phys. J. Special Topics **145**, 77–101 (2007)
© EDP Sciences, Springer-Verlag 2007
DOI: 10.1140/epjst/e2007-00149-0

THE EUROPEAN PHYSICAL JOURNAL SPECIAL TOPICS

The violin: Chladni patterns, plates, shells and sounds

C. Gough[a]

School of Physics and Astronomy, University of Birmingham, Birmingham B15 2TT, UK

Abstract. In this article we consider the vibrations and radiated sound of the bowed violin. The vibrations are discussed in terms of the normal modes of the instrument involving the coupled vibrations of the bowed string, the supporting bridge, the hollow shell comprising the body of the instrument and, ultimately, the acoustic modes of the performance space in which the instrument is played. We show that damping plays an important role in characterizing the normal modes in what can be distinguished as *weak* and *strong* coupling limits. The historic and modern application of Chladni pattern measurements to enhance our understanding of the acoustics and as an aid to the making of violins is highlighted, alongside the modern equivalents of experimental modal and computational finite-element analysis. The symmetry-breaking properties of the internal soundpost is shown to have a profound affect on the intensity and quality of sound radiated by the bowed instrument.

1 Introduction

After almost 150 years of research, understanding the acoustics of the violin and its relationship to the perceived quality of an instrument still remains a challenge. In part, this reflects the problem of understanding the acoustical properties of what is, in practice, a rather complex multi-resonant structure. But even more importantly – at least from the perspective of a scientist - because differences in acoustical properties must ultimately explain the widely believed superiority in the sound of violins by great Italian violin makers, like Amati, Stradivarius and Guarnerius and many of their contemporaries, with values often exceeding well over $1 M, compared with the sound of a typical $100 student violin and many, but certainly not all, modern instruments.

The violin first appeared in its present almost unchanged form in Northern Italy around the middle of the sixteenth century, with instruments from 1566 by Andrea Amati, the founder of the Cremonese school of violin making, still being played in the concert hall today. The outward form of the violin is a fine example of early Italian Renaissance design, with arching and convoluted outlines strongly influenced by the art, science and architecture of the period. Whether by art or design, the violin is a marvel of both ergonomic and acoustical perfection, which has met the requirements of the performing musician, musical styles and listeners, from the court and church in the late sixteenth century to the virtuoso soloists of today.

Figure 1 shows a *modern* (1846), nineteenth-century, copy by the leading French maker Vuillaume of a Guarnerius violin of around 1730. Vuillaume worked closely on the acoustics of the violin with the French scientist Felix Savart (1791–1841) – best known today for his work with Biot on establishing the mathematical relationship between electric currents and magnetic fields. As described later, Savart was one of the first to use Chladni pattern measurements as a serious scientific tool, in his pioneering researches on violin acoustics [2]. Chladni pattern

[a] e-mail: c.gough@bham.ac.uk

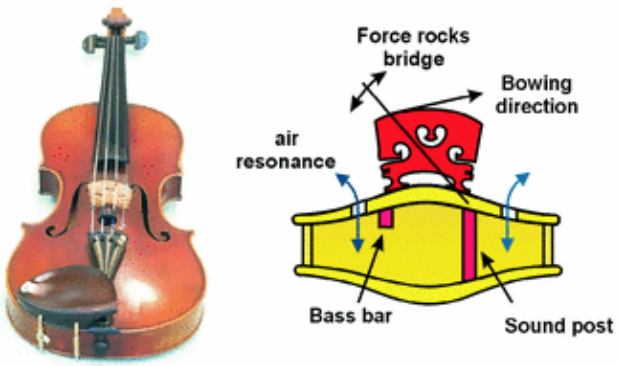

Fig. 1. A *modern* (1846) Vuillaume copy of a Guarnerius violin of around 1720 and a schematic cross-section of the violin body illustrating important internal features, the Helmholtz cavity resonance, and coupling of the bowed string to the vibrations of the body of the instrument.

measurements are still widely used by many violin makers, to monitor the frequencies and nodal lines of the modes of the individual plates of a violin, while being carved from the solid before the instrument is glued together.

Many other distinguished scientists have made major contributions to our understanding of the acoustics of the violin, pre-eminent amongst them being Helmholtz – the founder of modern acoustics. He was the first to understand the vibrations of the bowed string and the acoustically important resonance of the air inside the instrument, which vibrates in and out of the f-holes cut into the front plate, as described in the next section.

At the turn of the 20th century, C.V. Raman established his early scientific career with extensive and highly innovative experimental and mathematical investigations of the vibrations of bowed strings [22], before founding the Indian Physical and moving to America, where his research on opto-acoustics led to the award a Nobel Prize.

In more recent times, Frederick Saunders – known from Russell-Saunders LS spin-orbit coupling in atomic physics – was one of the first to attempt an understanding of the quality of a violin in terms of its acoustical properties [1]. With John Schelling, a retired research director from Bell Laboratories, and Carleen Hutchins, a biologist turned innovative violin maker, he co-founded the Catgut Acoustical Society of America. This society, through its newsletters, journal and meetings, established an international community of scientists, engineers and violin makers, with the aim of advancing our understanding of violin acoustics and the promotion of scientific methods as an aid to the more consistent and potentially improved quality of modern instruments.

Anyone interested in the acoustics of the violin should consult the four volumes of research papers edited and collated by Carleen Hutchins [3,4], who remains the inspirational leader of the scientific violin making community (see also, her comprehensive review of violin research prior to 1983 [5]). Cremer's monograph on the Violin [7] provides an authoritative guide by a leading researcher, while the advanced text-book on Musical Acoustics by Fletcher and Rossing [8] is an excellent source of the underlying science and provides references to most of the important research on the violin and many other instruments over the last century.

In this brief introduction, we adopt a physicist's viewpoint using simplified models and a normal mode and wave-functional approach, to describe the general principles underlying the production of sound by the violin and related stringed instruments. This approach differs from that of engineers, who aim to reproduce the acoustical properties using detailed structural and computational models, but often with less emphasis on general principles.

Section 2.1 provides a brief overview of the way that the bowed violin produces sound, following the chain of energy transfer from the bowed string to the larger acoustically radiating

surfaces of the shell of the instrument. We first describe (sec. 2.2) the excitation of bowed Helmholtz waves on the string. Such waves exert an approximately saw-tooth, periodic force on the bridge, which is very rich in harmonics, with amplitudes of the n-th partial varying as $1/n$. This results in a similarly periodic waveform of the sound radiated, but with amplitudes of the partials strongly dependent on the resonant frequencies and radiation efficiencies of the various structural modes excited–and the resonant modes of the performance space in which the instrument is played!

The bridge acts as a wide-band, but relatively strongly peaked, acoustic transformer facilitating the exchange of energy from the vibrating strings to the mechanical vibrations of the supporting body, as described in section 2.3. The coupling of the string vibrations to the resonant modes of the supporting body results in a set of normal modes. In section 2.4, we show that damping has a profound effect on the character of the normal modes in the cross-over region, where the resonances of the un-coupled systems would otherwise nearly coincide. We show that the normal modes can be classified as *weakly-* or *strongly-*coupled depending on the amount of damping present. This is a generic result for any set of coupled oscillators. The amount of damping present has a profound influence on the player's ability to control bowed notes, especially when the string resonates at a frequency close to an over-strongly coupled, weakly-damped, resonance of the main body of the instrument, resulting in what is known as the *wolf-note* [15,20].

Almost all the sound of a stringed instrument is radiated from the large area front and back plates of the shell of the instrument. The grading of the thickness and arching of such plates and the properties of the spruce and maple from which they are carved determine the frequencies and damping of the acoustically important vibrational modes of the body of the instrument. Such modes also include the coupled vibrations of the neck, fingerboard and tailpiece, as well as the air inside the cavity and all the other strings, whether bowed or not. Apart from the Helmholtz resonance discussed in section 2.5, involving the air inside the cavity vibrating in and out through the f-holes, none of these additional components are very efficient radiators of sound. However, they can all contribute significantly to the complex coupled normal modes of the instrument and can significantly perturb the frequencies and damping of string resonances. Such perturbations are particularly important, when any resonance of a component part coincides with prominent partials of the bowed string waveform. The coupling can then seriously affect the playability of the instrument. For the player, this may be just as important a factor as the tone quality in assessing the quality of an instrument.

The acoustical properties of the individual individual plates and main shell of the the instrument are discussed in sections 3 and 4. We briefly describe the way their acoustical properties are measured including Chladni measurements and modern equivalents like laser doppler interferometry and both computational and experimental modal analysis. In both sections, we examine the role of the geometric shape, f-holes, arching, bass-bar, soundpost and anisotropy of elastic constants on the the waveforms and modal frequencies. In section 5, we derive the modes of a Savart trapezoidal model of the violin using a finite element shell model, which illustrates why the soundpost and it's position plays such an important role in the sound of the violin and other members of the violin family. In sect. 6 we briefly consider the radiation of sound from the violin, the inherent difficulty of reliable assessment of violin quality and the difficulty of correlating such judgements with measured acoustical properties, followed by a very brief summary in section 7.

2 How the violin works

2.1 Overview

The violin produces sound by bowing one or more of the four strings stretched along its length, with the strings terminated at one end by the supporting bridge and at the other by the end-nut or the player's finger used to shorten the vibrating length and hence the pitch of the bowed note. The vibrating string – a linear dipole source – radiates a negligible amount of sound,

because its diameter is very much smaller than the acoustic wavelengths involved. To produce sound, energy has to be transferred to the radiating body of the instrument via the supporting bridge. The bridge is therefore never a perfect node of string vibration vibration, so that the harmonicity of the string modes is perturbed, as we will discuss in the next section.

The way that the transverse string vibrations are coupled to the main body of the instrument is illustrated schematically in fig. 1(b) showing a cross-section of the violin. The forces exerted by the two feet of the bridge, pressing against the central island region of the front plate, excite the vibrational modes of the main shell of the instrument. The front and back plates are strongly coupled by the supporting ribs and an asymmetrically placed sound-post wedged between between them, at a position close to the treble foot of the bridge. Without the soundpost the violin would, to a good approximation, be a symmetric structure. The couple acting on the bridge could then only excite asymmetric modes of vibration of the instrument, which at low frequencies would act as a rather weakly radiating dipole source of sound. Offsetting the soundpost results in additional coupling to the symmetric modes, which radiate more strongly as monopole sources. The soundpost and its position therefore play a very significant role in determining the intensity and quality of sound produced by an instrument (see Schelling [21]), as long recognised by French violin makers, who refer to it as l'âme or *soul* of the instrument.

At low frequencies, below around 400–500 Hz, there are no strongly radiating structural resonances. To boost the sound of the lowest notes, which extend a whole octave lower (down to 190 Hz), use is made of the cavity or Helmholtz air resonance at around 270–280 Hz. A similar resonance is used to boost the sound of the guitar at low frequencies, with the air vibrating in and out of the circular rose hole. In modern times, similar methods were used to boost the output of loudspeakers at low frequencies – the *bass-reflex* loudspeaker cabinet. Interestingly, insects like cicadas have been using such resonances to boost the sound they make [46] – for many millions of years.

The asymmetry of the violin is further enhanced by a tapered bass bar, which runs along much of the length of the violin close to the bass-side foot of the bridge. Its purpose is to strengthen the top plate, partly to resist the very large downward pressures exerted by the stretched strings, but acoustically more importantly, to increase the coupling of the central island section between the *f*-holes to the larger radiating surfaces of the top plate above and below.

2.2 The bowed string

The bowed string is excited via the visco-elastic frictional force of the rosin coating both the moving bow hairs and stretched strings [23]. The resultant waves excited on the strings are not the simple text-book sine waves generally used to illustrate wave motion on stretched strings, but are to a very good approximation Helmholtz waves. Helmholtz waves are transverse waves made up of any number of straight sections separated by kinks (discontinuities in slope) which, for a perfectly flexible string, travel around the string in either direction with the dispersion-less velocity of transverse waves $\sqrt{T/\rho}$, where T is the tension and ρ the density per unit length.

Such waves are just as acceptable solutions to the wave equation as are sine waves, with points on the the straight-line sections either at rest or moving with constant velocity, since within any straight section there can be no net transverse force. The only acceleration occurs as the kink moves between two straight sections moving with different velocities.

The bowed string waveform is the simplest Helmholtz wave, with a single kink moving around the string, separating two moving straight sections hinged about the rigid end supports. This is often referred to as a simple Raman wave, in recognition of Raman's pioneering experimental and analytical investigations of the bowed string [22]. To a first approximation, the string at the bowing point moves with the same velocity as the moving bow hair for part of the cycle, the *sticking* regime, and in the opposite direction with constant velocity for the remainder of the cycle, the *slipping* regime. This slip-stick motion is made possible because the frictional forces during the sticking regime are larger than when slipping.

Helmholtz waves with a single kink generate a periodic sawtooth-waveform force on the bridge, with the amplitude of the n-th Fourier component varying as $1/n$. The spectrum of sound produced by any bowed stringed instrument is therefore very rich in higher harmonics (~ 40 for the lowest notes on a violin or cello).

In the absence of damping or loss of energy from the reflecting ends, the Raman wave would persist indefinitely. In practice, the transfer of energy from the string to the vibrating surfaces of the instrument via the bridge results in a dynamic response at the point of bridge support and the generation of secondary waves. Together with reflections from the bow-hair, the secondary waves result in additional structure and degradation of the Raman waveform. Additional work has then to be done by the moving bow to maintain the slip-stick motion. Such processes were extensively studied by Lothar Cremer and his collaborators [7]. More recently, McIntyre and Woodhouse [9] at Cambridge and Schumacher [9,10], their American collaborator, have extended such investigations with computer-based models using a Green's function approach. Our current understanding of the bowed string has recently been reviewed by Woodhouse and Galluzo [12].

Detailed computational analysis of the slip-stick excitation mechanism have included such complicating factors as the finite flexibility of real strings, the excitation of the bowed transverse waves via the torsional motion of the string, dynamic reflections from both the bridge and bow, and the hysteretic visco-elastic properties of the frictional force. Despite such complications, which lead to small amounts of additional structure and a rounding of the waveform, the bowed waveform still approximates very closely to that of a simple Raman wave, as we will assume for the purpose of this article.

The quality of an instrument will therefore be determined by the overlap of the spectrum of the bowed string waveform with the multi-resonant response of the of the bridge, the body of the instrument and even the acoustic into which the sound is radiated, as illustrated in fig. 2. For illustration purposes only, we have separated the response of the bridge from that of the body of the instrument, though strictly speaking, we should always consider the coupled motions of all component parts of the instrument in terms of the collective normal modes. Because of the strong peaks and troughs in the multi-resonant response, the spectrum and hence waveform of the radiated sound varies dramatically from note to note – and even within a single note played with vibrato (frequency modulation) [13]. Surprisingly, although such variations may

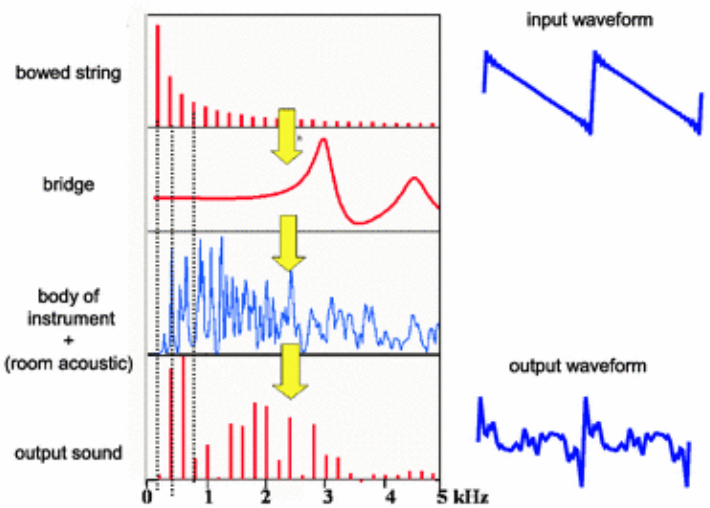

Fig. 2. A schematic illustration of the dependence of the sound of the violin on the input bowed waveform and spectrum and their modification by resonances of the bridge and body of the instrument. For simplicity the additional resonant structure of the performing acoustic has been omitted.

be responsible for much of the exciting quality of the sound of a violin, there is surprisingly little variation in the perceived quality in sound of an instrument from note to note or from point to point in the performance space. This demonstrates that the perceived quality of a violin is almost certainly associated with global features of the acoustic spectrum and not on the response at particular resonant frequencies, since the spectrum varies so dramatically from note to note, as is evident from fig. 2.

2.3 The bridge

Figure 1b illustrates the way that the transverse force from the bowed string excites the body of the instrument. At low frequencies the bridge can be considered as a rigid body with regard to the in-plane forces and induced vibrations. The transverse force of the vibrating string, polarised in the direction of the moving bow, exerts a couple on the central *island* region of the top plate between the *f*-holes via the treble- and bass-side feet of the bridge. Unless, by accident, the normal modes of the shell of the instrument simultaneously involve strong motions of both top and back plates, the essentially rigid sound post introduces a node close to the treble-side foot of the bridge. The bridge is therefore forced to rock about this point, with the bass-side foot of the bridge driving the central island region asymmetrically. As observed earlier, the asymmetrical excitation of the top plate results in the excitation of both symmetric, strongly radiating, monopole and asymmetric, weakly radiating, dipole plate resonances.

The rocking motion of the bridge at low frequencies will result in the point of string support moving at an angle relative to the bowing direction. String vibrations polarised in this direction will therefore be strongly coupled to the vibrations of the shell of the instrument, whereas vibrations polarised in the perpendicular direction will be essentially uncoupled. This leads to two independent modes of transverse string vibration, with one mode strongly perturbed in frequency and damping by coupling to the structural resonances and the other effectively unperturbed (Baker et al. [14]).

At higher frequencies, the main body modes generally involve significant vibrations of both the front and back plates, so that the soundpost post position will no longer be a node. The bridge then rocks on both its feet with the polarisation of the complex (in and out of phase components) admittance tensor at the point of bridge support varying strongly with frequency. In general, the string will support two orthogonal, elliptically polarised, modes of string vibration, with both modes damped by energy transfer from the string to the body resonances.

In addition, the bridge has its own important in-plane resonances involving the rocking and bouncing of the top part of the bridge on its two feet at typically around 3 and 6 kHz respectively. Such resonances strongly affect the reflecting impedance at the end of the string and the intensity, and hence quality of the radiated sound, as recognised by many early researchers (see [24] and [7, Chpt. 9]). This problem has recently been revisited by Woodhouse [25], to account for what is known as the BH (Bridge Hill)-feature or peak often observed at around 2–3 kHz in the frequency dependence of the admittance of the violin (induced velocity/force) measured in the bowing direction at the point of string support [26].

At the bridge resonance there is a broad peak in the admittance and radiated sound, with a peak height and width largely determined by the transfer of energy from the bridge to the shell of the instrument. Above the in-plane rocking resonance of the bridge, the motion of the top of the bridge is dominated by its inertial mass rocking about the waist of the bridge above its two supporting feet. The input admittance is then largely determined by the response of the bridge rather than by the body of the instrument, with an overall decrease in amplitude of 6 dB per octave. The amplitude of induced shell vibrations decreases even more rapidly, at around 12 dB per octave. Such a strong fall-off in response is responsible for removing much of the harshness of the sound generated by the sawtooth forcing waveform. This is easily demonstrated by the addition of an additional mass or mute to the top of the bridge. This lowers the frequency of the bridge resonance and results in an even softer sound, as often used by the player for special effect - *con sordini*. Despite such a well-known demonstration of the importance of bridge mass, many players–and sometimes even violin makers – are unaware of the importance of the bridge in affecting the overall quality of sound of an instrument.

2.4 Normal modes

Until now, we have discussed the vibrational modes of the instrument in terms of the separate vibrational modes of the strings, bridge and body of the instrument. However, as all readers of this article will be well aware, the coupled vibrations should really be considered in terms of the normal modes. The coupling of the transverse string modes to the structural modes provides an excellent example of the importance of damping on the character of normal modes [17], applicable to all coupled multi-mode systems.

As an illustrative example, we consider the simplest example of the transverse vibrations of a stretched string terminated at one end by a simple harmonic resonator, representing a coupled body resonance of the violin. We can characterise the coupled resonator vibrations by the terminating displacement v of the end support and the string vibrations by the amplitude u of the excited sinusoidal string vibrations. We then have a pair of coupled equations describing the motion of the coupled oscillator induced by the force exerted on it by the n-th string mode $(nT\pi/\ell)v$, with the resonator exerting a similar force on the end of the string, such that

$$M\left(\frac{\partial^2 u}{\partial t^2}+\frac{\omega}{Q_M}\frac{\partial u}{\partial t}+\omega_M^2 u\right)=\frac{nT\pi}{\ell}v, \tag{1}$$

$$m\left(\frac{\partial^2 v}{\partial t^2}+\frac{\omega}{Q_m}\frac{\partial v}{\partial t}+\omega_m^2 v\right)=\frac{nT\pi}{\ell}u, \tag{2}$$

where M, ω_M and Q_M, and m (half the mass), ω_m and Q_m represent the effective masses, resonant frequencies and Q-values of the coupled oscillator and string, length ℓ and tension T.

In the absence of damping, we recover the familiar result, with normal modes split at the crossing point such that $\Omega_\pm^2=\Omega_o^2\pm\triangle^2$, where

$$\triangle^2=(nT\pi/\ell)\sqrt{1/mM}=\frac{4\omega_M^2}{n\pi}\sqrt{\frac{m}{M}}. \tag{3}$$

At the crossing point, the normal modes can be described as a combination of string and coupled oscillator vibrations, with equal energies and amplitudes either in or out of phase. On passing through the cross-over region, the normal modes vary smoothly from being predominately string-like to that of the coupled oscillator – and vice versa, with both modes damped by half the damping of the coupled mode. This is the classical equivalent of mode splitting in wave-mechanics, where elementary texts generally ignore the effects of damping, which can considered as coupling to a broad spectrum of other modes.

In classical systems, damping is always important. In the absence of intrinsic string damping, the complex frequencies of the damped normal modes are given by

$$\Omega_\pm^2=\omega_+^2\pm\{\omega_-^4+\triangle^4\}^{1/2} \tag{4}$$

with, to first order in damping,

$$\omega_\pm^2=\frac{1}{2}[\omega_M^2\pm\omega_m^2+\mathrm{i}(\omega_M^2/Q_M)] \tag{5}$$

and $\mathrm{i}=\sqrt{-1}$.

At the crossing-point, where the uncoupled resonances coincide, the frequencies of the coupled normal are given by

$$\Omega_\pm^2=\left[\Omega_M^2(1+\mathrm{i}/2Q_M)\pm(\triangle^4-(\Omega_M^2/2Q_M)^2\right]^{1/2}. \tag{6}$$

There is clearly a transition in character of the normal modes as the damping is increased leading to the bracketed second term on the right-hand side of eq. (6) becoming negative. When this occurs the splitting in frequency of the modes disappears and is replaced by a splitting in the damping at the cross-over frequency. This occurs when

$$K=\frac{4Q_M}{\pi}\sqrt{\frac{m}{M}}=1 \tag{7}$$

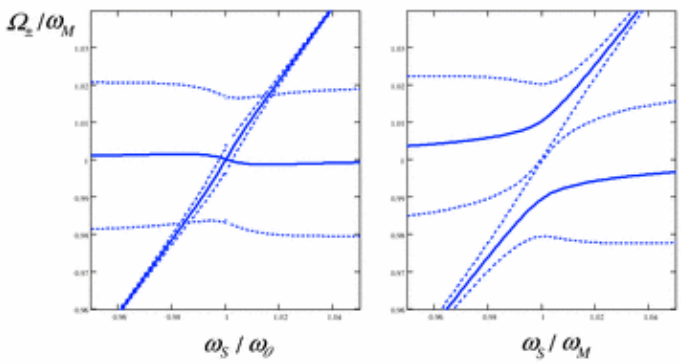

(a) $K = 0.72$ (b) $K = 1.45$

Fig. 3. The frequencies $\Omega_\pm$ of the damped normal modes of an undamped string coupled to a damped body resonance with $Q = 25$ as a function of string frequency ω_S passing through the cross-over region, for (a) weak-coupling $K = 0.72$, and (b) strong coupling $K = 1.45$. The solid curves show the frequencies of the damped normal modes and the dashed curves indicate their 3-dB widths, with all frequencies normalised to that of the coupled resonator Ω_M.

The difference in behaviour in the *weak* ($K < 1$) and *strong* ($K > 1$) coupling limits is illustrated in Fig. 3. The solid curves represent the frequencies of the coupled modes and the dashed curves mark their 3dB widths. In the weak-coupling limit, when the damping width of the coupled body mode is larger than the splitting would have been in the absence of damping, there is no splitting of the normal modes. The modes retain their predominantly string-like or coupled resonator characteristics throughout the cross-over region, with a small dispersion in the frequency of the *string* resonance and increase in its damping in the cross-over region. Conversely, in the strong-coupling limit, when the splitting is larger than the damping, the modes are split in the cross-over region and one can no longer refer to the modes as essentially string-like or body-like in character, being a combination of both. Note the relatively small change in coupling constant required to produce a dramatic change in behaviour in the cross-over region.

The above analysis is quite general for any damped classical or quantum mechanical system. It justifies treating the various components of a complicated multi-resonant structure like the violin (e.g. string, bridge, neck, fingerboard, shell, and cavity modes) as individual resonators, which are only weakly perturbed by their interactions, provided the damping of the coupled modes is larger than their interaction strengths Δ^2. However, such an approximation breaks down, for example, when the strings on a violin are over-strongly coupled to a lightly damped body resonance, leading to a split pair of normal modes at the cross-over region. This destroys the harmonicity of the string modes, so that it is no longer possible to establish a freely propagating Helmholtz-wave on the bowed string.

This is the origin of the infamous wolf-note phenomena, which causes a breakdown of the sound of a bowed string when the fundamental component of the string vibrations coincides with a strongly excited resonance of the body of the instrument [15,16]. The coupled motion results in a split pair of coupled modes (by as much as 10% on some cellos), removing the fundamental component of the Helmholtz wave, but leaving the higher partials largely unperturbed. The string therefore tends to make transitions to a new Helmholtz wave an octave higher based on the even harmonics of string vibration, which makes the note very difficult for the player to control. An important aspect of the violin's design is to maximise the coupling of the string to the radiating shell modes, without the coupling becoming so strong that it destroys the harmonicity of string vibrations.

To overcome such problems, one can attempt to reduce K by using a lighter string, increasing the effective mass of the coupled resonance by moving the position of the sound

post, or increasing the damping of the troublesome coupled resonance (sometimes a cork or duster wedged between the tailpiece and front plate can have the desired effect. An alternative solution is to transfer energy to a similarly tuned but *lossy* resonator. A heavily damped mass fixed to one of the strings on the non-bowing side of the bridge is frequently used, or a damped cantilever resonator mounted inside the instrument.

2.5 Cavity air resonances

The lowest efficiently radiating structural modes of the main body of the instrument for a violin are typically between 450 and 500 Hz – more than an octave above the lowest notes played on the instrument. This is true for all members of the violin family as well as for the guitar. To help boost the sound output at lower frequencies, use is made of the Helmholtz resonance involving the oscillation of the air inside the hollow body of the instrument in and out via the *f*-holes. For a rigid cavity, the Helmholtz resonance frequency is given by

$$\omega_H = c\sqrt{\frac{S}{\ell V}}, \tag{8}$$

where c is the speed of sound in air, S the area of the *f*-holes and ℓ their effective length, treated as the neck through which the air enters and leaves the cavity; ℓ is a shape-dependent factor of order the typical slot-width of the *f*-hole openings [7, sec. 2.3]. In practice, the Helmholtz resonance on a violin is typically 270–290 Hz, boosting the sound output for notes around the 2nd-lowest open string.

The Helmholtz resonance is driven by any *breathing* mode of vibration of the shell of the instrument involving a net change in volume of the enclosed air. These will also be the most strongly radiating modes. Because the frequencies of the Helmholtz resonator and the most important shell modes are well separated, the coupling is relatively weak, slightly lowering the frequency of the Helmholtz air-resonance and raising the frequency of the coupled body resonances - as expected from our earlier discussion of coupled resonators illustrated in fig. 3.

Because the Helmholtz resonances involves a bulk motion of air in and out of the body of the instrument, it acts as an efficient monopole radiator of sound. However, for excitation at frequencies below the Helmholtz cavity resonance, any net changes in volume of the shell of the instrument will be exactly compensated by air moving in or out of the cavity. Hence very little sound is radiated at the fundamental frequency of the lowest notes, though the radiated waveforms remain periodic, with almost all the sound intensity concentrated in the higher partials. This illustrates the well-known *missing fundamental* phenomenon in perceptual acoustics, whereby the perceived pitch of a note is determined by the periodicity of the waveform, whether or not there is a fundamental component present.

In addition to the Helmholtz resonance, there are a large number of quasi-2-dimensional resonant modes of the air within the cavity (Jansson [27] identified around 30 such modes below 4 kHz). Such modes are generally only weakly coupled to the resonances of the shell of the instrument, but may nevertheless radiate a significant amount of sound through the *f*-holes. The contribution of such modes to the the sound of the violin remains unclear.

3 Plate modes

3.1 Measurements

We now consider the vibrations of the body of the instrument made up of the top and back plates, the supporting ribs, the fingerboard, neck, tailpiece and any other attached objects like a shoulder-rest or chin-rest. But first we consider the plates separately, as they are undoubtedly the most important components of the violin in determining the quality of the sound produced.

The top and back plates are cut from solid wedges of spruce and maple respectively. The plates can support longitudinal, flexural and torsional modes of vibration. Of these the flexural

and torsional are the only motions that involve acoustically radiating displacements perpendicular to the surface of the plates. The acoustic properties of the plates are determined by their geometric shape, the density and elastic properties of the wood, variations in thickness across the plate and geometric arching. It is the maker's skill in controlling all such parameters, taking into account the inevitable variation in density and anisotropic elastic properties of the particular plank of wood from which the plates are carved, that determines the acoustical properties and ultimately the quality of sound of the assembled violin.

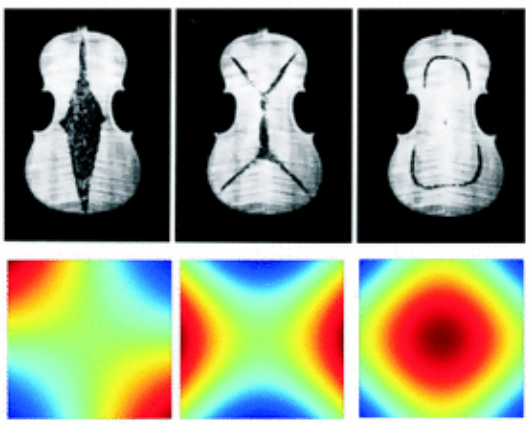

Fig. 4. Chladni patterns for the first twisting (#1) and bending X- and ring-modes (#2 and #5) of a viola back plate (from Hutchins) and the related modal patterns for an isotropic square plate. Equal amplitudes of vibration are indicated by different colours (e. g. from red-positive to blue-negative).

Makers continuously test the elastic properties of the plates as they thin them down from the solid. Traditionally, this was done by feel, as the plates were flexed and twisted by the hands, and by listening to the sound when they were tapped or rubbed around the edges by the thumb. More recently, largely inspired by Carleen Hutchins and her followers [19], many modern makers use more quantitative, scientific measurements to monitor the modal frequencies and modal line-shapes of the individual plates as they are carved from the solid. From the observed changes in frequencies and nodal line shapes on selective thinning in particular regions, the maker continuously refines the thickness gradations across the plates. The aim is to end up with prominent free-plate modes having a particular set of final frequencies and well-defined nodal line shapes.

Chladni pattern measurements still provide provide the simplest, most convenient and least expensive way of making such measurements. To obtain Chladni patterns, the plate is lightly supported at the nodal points of the particular mode to be measured and is placed over a loudspeaker cone driven by a sine-wave oscillator. Christmas glitter or some other such light material is sprinkled over the surface. When the frequency of the sound from the loudspeaker strongly excites a resonant mode, the glitter moves to the nodal line positions.

Figure 4 shows Chladni patterns for a freely supported viola back plate illustrating the three modes that tend to be used in the gradation of thicknesses. The corresponding modes of a freely supported isotropic square plate are shown for comparison. In both cases the first mode is a simple twisting mode. The following two modes are flexural or bending modes and are referred to as the *X*- and *ring*-modes in view of their similarity with the modes of the square plate. Such modes can be considered as combinations of [10] and [01] modes, which for a stretched membrane would be degenerate. However, when a thin plate is bent in a given direction, it bends in the opposite sense in the orthogonal direction (anticlastic bending). This is a consequence of the Poisson effect relating longitudinal extensions to transverse contraction when a plate is

stretched. This lifts the degeneracy of the two illustrated modes, with the X-mode with the inherent anticlastic bending in opposite directions having the lower potential energy and hence lower modal frequency than the *ring* mode, with bending in the same sense in both directions.

Savart, working closely with Vuillaume in the the early part of the nineteenth century, noted that the plates of fine Italian violins had strong plate resonances between C♯4 and D4 (∼280–300 Hz) for the front plate and between a semitone or tone higher for the back plate (Savart [47]), observations that were subsequently confirmed in measurements by Hutchins and Saunders on a large number of violins [6]. Hutchins has also suggested that the early Italian master violin makers may well have tuned the modes of their freely supported plates to ring like a well-tuned bell, with the frequencies of the lowest free-plate modes in simple harmonic relationship to each other. A bell-like ring would be optimised when the frequencies of modes #1, #2 and #5 of the top plate are close to an octave apart. In addition, she aims to closely match modes #2 and #5 in the front and back plates, though mode #1 cannot then be matched, because of the different geometry of the top plates (i.e. with *f*-holes and bass bar). In addition, she advocates adjusting the thicknesses of the plates to yield well-defined, symmetrical, Chladni nodal-line patterns, similar to those shown in fig. 4.

Such design criteria clearly go well beyond what the skilled Cremonese maker's could possibly hope to have achieved by feel and sound alone – though the ability of skilled violin-makers using their fingers, ears and experience alone to assess and interpret the feel and sounds of plates should never be underestimated. However, because they needed to make instruments as quickly as possible to satisfy their customers and optimise their income, it is far from clear that Cremonese makers would have spent the time in making such careful matches, even had the scientific tools then been available. Nor is it clear, that instruments made using these scientific tools are necessarily any better than instruments made by more traditional methods. However, such methods will provide a degree of quality control on the overall acoustic properties that should, at the very least, lead to a more consistent quality of instrument.

Unfortunately, there is relatively little reliable published information on the vibrational modes of the free plates of outstanding Cremonese instruments, as modern players and dealers are naturally unwilling to allow their valuable instruments to be taken apart for such measurements. However, such measurements were performed on many fine instruments by Savart and Vuillaume, probably while the instruments were being taken apart, modified and reassembled to *improve* their tonal properties, to match the demands of the the virtuosi performers and larger concert halls of the day. The improvements included lengthening the neck, using higher tension metal-covered rather than gut strings, increasing the slope of the strings over the bridge, using a thicker bass bar, a larger diameter soundpost, a modern bridge, and sometimes even adding and removing wood from the plates themselves. As a consequence, the powerful and rich sounds of today's *modernised* Cremonese instruments are very different from the quieter and sweeter sounds of the instruments actually made by Amati, Stradivarius, Guarnerius and their contemporaries. The paradox is that we are attempting to discover the apparent *secret* of how the great Italian makers made instruments with such outstanding tonal qualities in the concert hall today, whereas when they were made they sounded very different.

3.2 Thin plate theory

Understanding the beautiful Chladni patterns generated on differently shaped plates presented a formidable challenge. In 1809 Napoleon offered a prize of 3000 francs for the first person to provide a theory for such vibrations. The prize was eventually won in 1816 – at her third attempt – by Sophie Germain, though a complete theory was not obtained until 30-years later by Kirchhoff [49].

Equation (9) is the fourth-order wave-equation describing flexural or bending waves in a thin plate. The equations have been generalised to account for the highly anisotropic properties of the wood used for the plates of stringed instruments (see [28]). In these applications, the

wood is aligned with the grain running along the length of the instrument, making it far easier to bend in the transverse direction, across the grain.

$$\rho t \frac{\partial^2 u}{\partial t^2} + B_{xx} \frac{\partial^4 u}{\partial x^4} + 2B_{xy} \frac{\partial^4 u}{\partial x^2 \partial y^2} + B_{yy} \frac{\partial^4 u}{\partial y^4} = 0 \tag{9}$$

with

$$B_{xx} = \frac{E_{xx} t^3}{12\rho(1-\nu_{xx}^2)} \qquad \text{and} \qquad B_{yy} = \frac{E_{yy} t^3}{12\rho(1-\nu_{yy}^2)} \tag{10}$$

and

$$B_{xy} = B_{yx} \sim (B_{xx} B_{yy})^{1/2}, \tag{11}$$

where t is the local plate thickness and E_{ij} and ν_{ij} are the anisotropic elastic constants and Poisson ratios along the symmetry directions parallel to the x- and y-axis.

Well away from the boundaries or any localised boundary condition like the presence of the soundpost, a thin plate supports sinusoidal waves with frequencies

$$\omega \simeq t \sqrt{\frac{E_{xx}}{12\rho(1-\nu_{xx}^2)}} \left(k_x^2 + \sqrt{\frac{1}{\alpha}} k_y^2 \right), \tag{12}$$

where k_x and k_y are the wave-vectors along the symmetry directions and $\alpha = B_{xx}/B_{yy}$ represents the anisotropy of the elastic constants. For typical sitka spruce soundboards of keyboard instruments and the front-plates of the violin or guitar, the anisotropy is along relative to across the grain is very large, with α ranging from around 13 to 24 (see [8, pp. 721–2]). Within the approximation assumed in eq. (11), the flexural modes of an anisotropic plate of any shape can be deduced from an equivalent isotropic plate with elastic constant the geometric mean of the anisotropic plate and the x- and y-lengths scaled by the factor $\alpha^{1/8}$ (1.4–1.5) and its inverse, keeping the plate area constant. The dispersion relationship leads to an average constant density of states for flexural waves at high frequencies, with a typical spacing of about 70 Hz for a violin front plate and 110 Hz for the back plate [7, p. 292]. However, damping causes considerable overlap of the resonances, so that the partials of the bowed string input tend to excite groups of closely-spaced structural modes simultaneously.

In addition to propagating wave-like solutions, the fourth-order partials in the wave equation also allow exponentially damped solutions varying as $e^{\pm k_x x}$ and $e^{\pm k_y y}$ with the same dispersion relationship. Such solutions are important at the edges of the plate and have to be included to satisfy the boundary conditions, unless the plate is hinged at its edges. For a free plate, the boundary conditions require the forces and couples acting on the edges to be zero, which mixes flexing in the x- and y-directions. Unlike the simple straight-line nodal patterns of transverse waves on a stretched rectangular membrane, such mixing results in considerable curvature of the modal lines, which accounts for many of the beautiful shapes observed in Chladni patterns.

Thin plates also support torsional modes, such as the twisting, $u = xy$, mode #1 in fig. 4. Unlike the bending modes, these modes are non-dispersive with a wave velocity $c_T = (2h/w)\sqrt{E/2\rho(1+\nu)}$ for a thin plate of width w, where the elastic properties will again be affected by anisotropic shear moduli parallel to and across the grain. For a freely supported thin-plate, conservation of linear and rotational momentum and boundary conditions can induce coupling between the bending and torsional modes, demonstrated later in relation to shell modes.

3.3 Plate geometry

The modes of the violin are strongly influenced by the outline of the individual plates, the *f*-holes cut into the top plate and the strengthening bass-bar [30]. Because the plates are relatively rigidly supported by the side ribs, the wave functions and corresponding frequencies will be very different from those of the freely supported plates tested by the maker in the

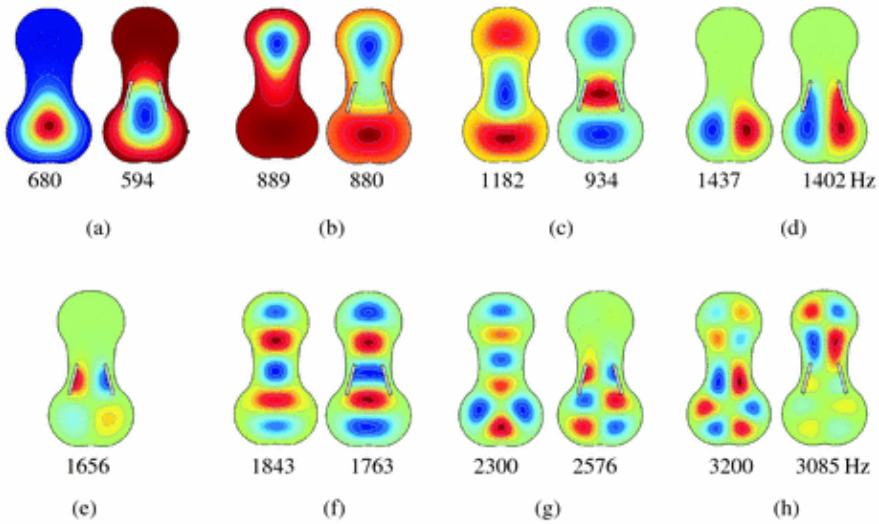

Fig. 5. (a)–(h) Selected modes of an isotropic, flat, guitar-shaped, thin plate before and after cutting slots to mimic the effect of *f*-holes.

pre-assembly stage. The relatively narrow waist of the plates tends to separate the upper and lower areas, so that at low frequencies several modes can be excited that are predominantly localised in the upper or lower sections. This is illustrated in fig. 5 by selected modes of a guitar-shaped flat plate, rigidly supported around its edges, before and after slots are cut into the plate to mimic the effect of the *f*-holes. The modes were calculated using COMSOL [38], a powerful but user-friendly software package for rapid finite-element calculations. This software is particularly useful for illustrating the vibrational modes of simple structures – as in this article – though its real strength lies in multi-physics modelling of complex structures.

The size and shape of the plate in the above example was been chosen to approximate to the geometry of the major vibrating surfaces of actual violin plates (a smoothed guitar-shaped region following the line of the ribs and the inside of the solid wooden blocks that strengthens the shell at the corners above and below the waist. At this stage, no attempt has been made to to incorporate the arching of the plates or the appropriate orthotropic elastic properties of the wood. Although such factors will affect the detailed shape and frequencies of modes, their inclusion would not be expected to change the basic physics illustrated by this simplified model.

The modes in figs. 5(a), (b) and (d) illustrate the tendency for localisation of the vibrations into the upper and lower regions of the plate. For these examples, the presence of the slots, with their freely supported edges, allows an increased penetration of the wave-functions into the relatively flexible central island section on which the bridge rests. This not only lowers the modal frequencies but, more importantly, significantly increases the strength of the coupling of such modes to the vibrating strings – via the bridge resting on the island section. This will clearly increase the intensity of the radiated sound. The shape and position of the *f*-holes is therefore likely to be important important, not only for their role in determining the frequency of the Helmholtz air resonator boosting the low-frequency response, but also for allowing modal vibrations to penetrate more strongly into the island region supporting the bridge.

One can consider the island region between the slots or *f*-holes as a 3-port acoustic transformer coupling the modes of the upper and lower regions of the plate, as in fig. 5(c), (f), (g) and (h), in addition to coupling such vibrations to the vibrating strings via the bridge. At certain frequencies, the coupling between the upper and lower regions can be large, as in fig. 5 (c), (f) and (g – without slots), or relatively weak, as in fig. 5(h), where the coupling with and without the slots reverses the relative amplitudes of the modes in the upper and lower regions. From our discussion of coupled oscillators (section 2.4), one expects the coupling

strength to be strong when the resonant frequencies of the modes in the upper and lower regions of the plate are closely matched, but weak otherwise. In addition, the island region can have resonant modes of its own, as illustrated in fig. 5(e) and (g – with slots), which have no parallel in the unslotted plate. Such modes, with antinodes of vibration at the slot or *f*-hole edges, arise because of the increased flexibility of the freely supported central island region relative to the rigidly supported region without slots.

3.4 Soundpost

For symmetrical plates, the symmetry of the coupled wave functions in the upper and lower regions will always be the same (i.e. either both odd or both even about the central axis). However, in the assembled instrument, the offset soundpost wedged between the two plates introduces an additional asymmetric constraint. At low frequencies, the modes of the front and back plates are generally well separated. This results in the soundpost position acting as a node of vibration, because the soundpost is a rather rigid body with its longitudinal mode resonances at very much higher frequencies. A node at the position of the soundpost can only be achieved by combinations of the symmetric and asymmetric modes illustrated in fig. 5. This often results in rather complicated modal wavefunctions, especially at high frequencies, as in fig. 6(d – with soundpost). The combined modes will tend again to be those with closely matching frequencies.

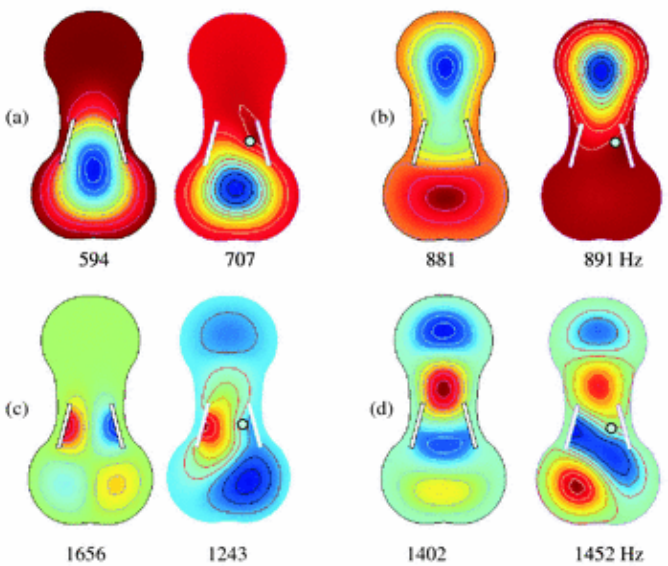

Fig. 6. (a)–(d) Modal wavefunctions and frequencies for a guitar-shaped thin plate with slots, with and without a soundpost - position indicated by the solid circles.

Figure 6(a–d) illustrates the effect of an offset soundpost on some of the lower frequency modes, with wave-functions forced to move away from the soundpost nodal position and readjusting their distribution across the plate to minimise their stored energy. The perturbation of the wavefunctions results in a highly asymmetric local region of the wavefunction in the island region. When incorporated into the body of the instrument, such modes would allow the *asymmetrical* rocking motion of the bridge to couple strongly to the *symmetrical* lowest order modes of the plate, fig. 6(a) and (b), which provide strong sources of monopole radiation. The node at the soundpost will also strongly perturb any modes localised to central island region localised modes, fig. 6(c).

3.5 Bassbar

The asymmetry of the front plate of a violin is further enhanced by the bass bar, which increases its ability to support the downward force of the stretched strings on the bridge without collapsing. It also affects the vibrational modes by increasing the coupling between the upper, lower and island regions. However, because its mass is relatively small compared with the plate itself, it only weakly perturbs the modal frequencies, as indicated for the first four modes in fig. 7. Nevertheless, it increases slightly the penetration of the wavefunctions into the island region and proximity to the bridge and will therefore increase the output sound somewhat.

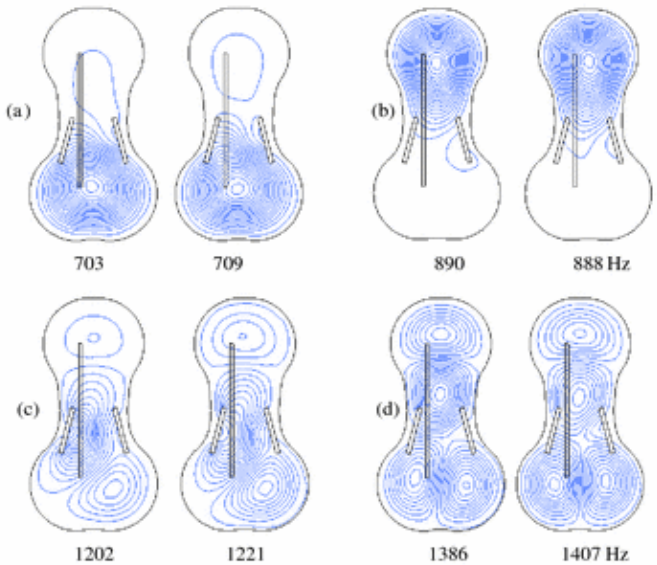

Fig. 7. (a)–(d) First four modes of guitar-shaped thin plate with slots and a soundpost node, with and without a 5×5 mm rectangular bass bar in the position indicated.

3.6 Arching

The beautiful arching of the front and back plates of the violin was almost certainly chosen to prevent the body of the instrument from collapsing under the large downward force of the stretched springs pressing on the top plate. However, more importantly from an acoustics viewpoint, such arching results in a significant increase in modal frequencies, particularly for the lowest order bending modes. This arises because any motion of the plates perpendicular to an arched surface induces a first-order longitudinal strain parallel to the surface. This increases the potential energy and hence frequency of the flexural wave modes. The perturbation is larger for symmetric modes than for asymmetric modes, where the net energy change in potential energy is much smaller. The effect of arching also decreases with increasing frequency, as the wavelengths of the of the flexural vibrations become much shorter than the characteristic radii of curvature.

As an example, the fundamental mode of a circular plate, belled outwards to a height H, is initially increased by a factor $\sim [1 + \alpha(H/h)^2]$, where $\alpha = 0.67$ when clamped at its edges and 0.84 when freely supported [29]. For the violin, with a typical front-plate thicknesses of around 2.5–3.5 mm and arching heights in the range ∼13–16 mm, this would imply an approximate doubling or more of the frequency of the lowest order flexural mode relative to that of a flat plate. This is consistent with finite element analysis computations of the modes of a freely

supported arched violin plate by Roberts [30], yielding a 3-fold increase of some modes on varying the arching from zero to twice the normal height.

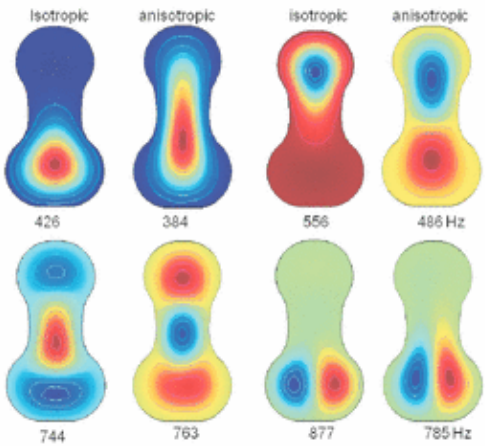

Fig. 8. Modal waveforms and frequencies of guitar-shaped thin plates with isotropic and anisotropic elastic constant, as described in the text.

The frequencies of the lowest important acoustic modes can therefore be just as dependent on the arching height and the arching contour as on plate thickness [30,36,37]. The reduction in the arching height of violins from the highly arched Stainer and early Amati models to Stradivari violins and even flatter Guarneri models is almost certainly the main reason for the increased intensity and darker sound of the latter instruments.

3.7 Anisotropy

The violin front plate is generally made of sitka spruce and the back from maple, both of which have highly anisotropic elastic properties parallel and transverse to the grain running along the length of the the plates. As described earlier, one can use isotropic thin plate theory to evaluate the modes of anisotropic materials by scaling the geometry parallel and perpendicular to the grain by the factor $(E_L/E_T)^{1/8}$ perpendicular to and its inverse along the grain, using an elastic constant equal to the the geometric mean $\sqrt{E_L E_T}$ of the anisotropic elasticity constants. Such scaling leaves the density of modes unchanged at high frequencies. Having determined the modal waveforms and frequencies, one can then reverse the scaling, to view the waveforms in the original geometry.

This is illustrated in fig. 11, which compares the first four modes of guitar-shaped plates, first for an isotropic plate with the geometric mean of the elasticity constant and then for an anisotropy factor of 10. The increase in elastic constant along the grain for the anisotropic plate leads to a significantly larger penetration of the first mode into the island and upper regions of the plate, and an associated decrease in the modal frequency from 426 Hz to 384 Hz. Whereas the first mode of the anisotropic plate can be considered as having a large contribution from the first two modes of the isotropic plate acting in phase, the second mode is clearly a combination of the two modes with opposite phases and a corresponding frequency of 486 Hz in between them (426 and 556 Hz). In contrast, the anisotropy has only a slight influence on the wavefunctions and modal frequencies of the third mode, whereas the anisotropy significantly lowers the frequency of the fourth mode, due to the greater penetration of the waves into the central region.

In general, the larger the degree of anisotropy the larger will be the coupling of the major plate vibrations into the island area on which the rocking bridge rests. This explains why the

acoustical properties of the individual plates and shell of the instrument are so sensitive to the elastic constants and anisotropy of the wood from which they are carved. In practice, makers go to considerable lengths in the selection of the wood they use, which varies from species to species, tree to tree and the local climatology – even from which side of the tree the wood is taken. Recently is has been suggested that the claimed superiority of Cremonese instruments is derived from the quality of the wood that was available to the great makers [42], but this remains a contentious issue.

4 Shell modes

4.1 General considerations

Having discussed the properties of the individual plates in some detail, we are now in a position to consider the modes of the assembled body or shell of the instrument. The normal modes of the shell of the instrument will include the vibrations and coupling of the plates, the supporting side ribs, the soundpost and air inside the body. In addition, the vibrational modes of the neck, fingerboard and tailpiece will be also be involved, though they may not themselves be responsible for significant acoustic radiation [32]. Because the fingerboard and neck are attached to the outer edges of the violin, where the amplitude of the excited modes is generally relatively small, to a first approximation, we can ignore such attachments. They can be included later as weakly coupled resonators, with their own modes adding to the normal modes of the assembled instrument, only weakly perturbing the shell modes.

In addition, in any measurements or when played, the instrument has to be supported (e.g. by the shoulder- and chin-rest and the hand supporting the neck). Because such supports are again made via the edges of the shell, the resulting perturbation of the normal modes will be relatively small. In practice, the main effect of holding an instrument is to increase the damping of any shell mode involving significant motions of the outer edges at the positions of support [13,32,40].

The normal modes of a shell will include the six displacement and rotational motions of the body of the constrained instrument. In addition there will be plate-like twisting or twisting motions of the main shell of the instrument about the 3 principal axis, just like the torsional modes of a thick plate. Then there will be the flexural motions of the plates largely responsible for the radiated sound. For a freely supported shell, the flexural modes can couple to the translation, rotational, twisting and flexing modes of the structure as a whole.

Fig. 9 shows selected modes of a simple rectangular box with all surfaces having the same properties and thickness, which illustrate the coupling (or lack of coupling) of the flexural waves to the other degrees of freedom. The first example at 310 Hz, is the major breathing mode, with the front and back plates vibrating in their fundamental mode, but in opposite directions. The two plates therefore exert equal and opposite forces and couples on the supporting side structures. As the coupled bending modes of the sides will have high modal frequencies, because of their relatively small height, they will act as rather stiff springs. This will inhibit any significant rotation about the plate edges. For this particular mode, the shell mode and modal frequency will therefore approximate rather closely to those of rigidly supported top and back plates. This will be an increasingly valid assumption at high frequencies.

In contrast, for plate vibrations in the same sense in the front and back plates, there will be significant coupling to the translational, rotational and twisting modes of the overall structure, as illustrated by all the other selected examples in fig. 9. However, apart from the strong anticlastic bending mode at 1216 Hz, the displacements of the side-walls are generally small compared to the major excursions within the top and back plates, as illustrated by the modal patterns of the front plate alone.

Similar arguments will hold for the violin. However, because the front plate is somewhat thinner than the back plate and has an increased flexibility due to the *f*-holes, the modal frequencies will be lower than in the back plate and the density of modes correspondingly higher. Moreover, for a given exciting force the displacement will also be smaller. The acoustic

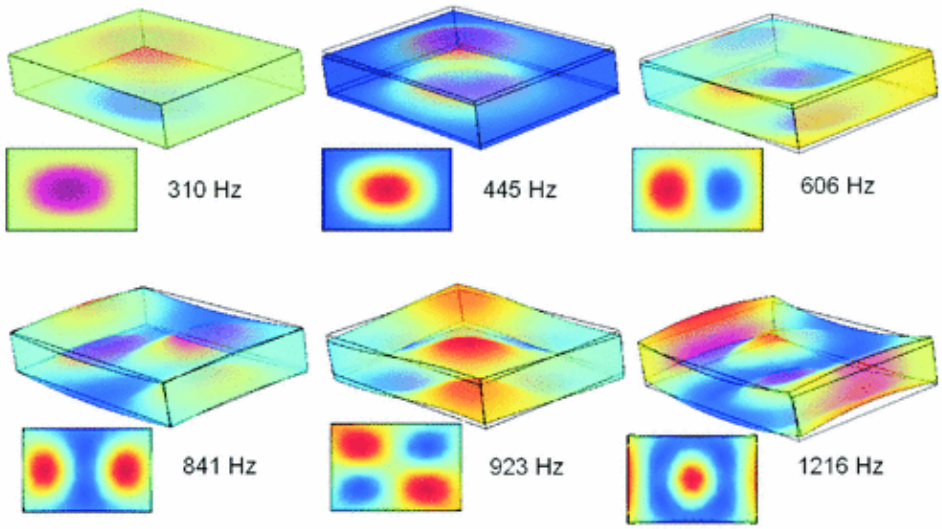

Fig. 9. Examples of shell modes of a freely supported rectangular box (5×3×2) with walls of equal thickness, chosen to illustrate the interaction of the flexural plate modes to the translational, rotational, twisting and bending modes of the structure as a whole. The first mode involves vibrations of opposite sign in the top and back plates, in all others the front and back plate move in the same direction. The individual plate modes are illustrated.

properties and quality of the violin are therefore likely to be more strongly influenced by the properties of the front plate than the back, though the latter is still responsible for a significant fraction of the radiated sound.

Because the edges of the front and back plates of the violin are supported fairly rigidly by the supporting ribs, it could be argued that makers might find it more helpful to optimise the modal frequencies and nodal line shapes of plates, with the plates glued round their edges to a rather rigid supporting structure. This would then more closely approximate to the modes of the shell of the instrument when assembled than the freely supported plates most usually considered.

4.2 Modal analysis

Unfortunately, it is not possible to perform Chladni measurements on the highly arched surfaces of the violin. However, equivalent measurements can be made by frequency- and time-domain laser holography [36] and by both computational (see Knott [31], Rogers [37] and Roberts [30]) and experimental modal analysis (Marshall [40] and Bissinger [32]).

Figure 10(a) shows two projections of a normal mode of a violin obtained from finite element analysis computations by Knott [31]. The amplitudes of vibration are greatly exaggerated for illustration purposes. In practice, they are typically of order microns, so one is well within any linear limit elastic approximation. Such computations show that many of the modes involve significant vibrations of the neck, fingerboard and tailpiece. A particular advantage of finite element analysis is the ability to investigate the effects of varying the materials and design of a violin at will, without having to build and test a new instrument.

In experimental modal analysis, the instrument is excited at some point, such as the top corner of the bridge, and the induced vibrations measured at a large number of points (typically ∼40) distributed over the surface of the instrument. The induced velocities can, for example, be monitored by laser doppler measurements, (see Bissinger [32]). Figure 10(b)

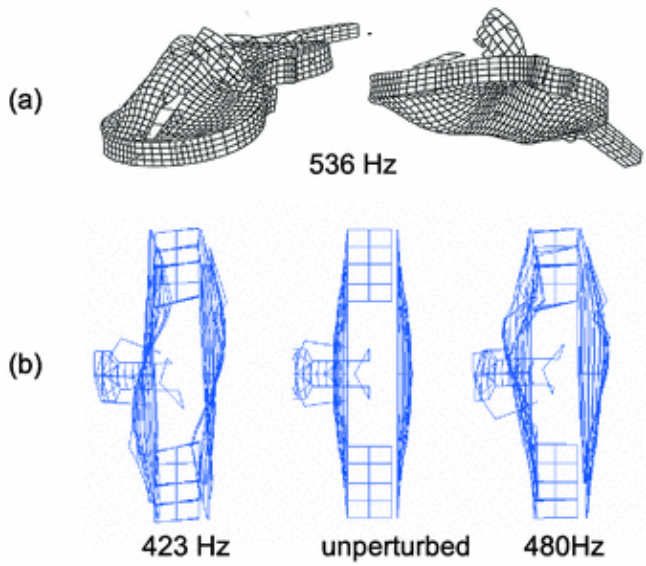

Fig. 10. (a) Two views of exaggerated displacements of an important breathing mode at 536 Hz for a computer-modeled violin derived by Knott [31] using FEA, and (b) a "see-through" cross-section of displacements of a weakly radiating mode at 425 Hz and a strongly radiating breathing mode at 480 Hz for a real violin obtained from experimental modal analysis by Bissinger [44].

shows a *see-through* cross-section of two strongly excited modes of a violin at 423 and 480 Hz obtained from such measurements. Alternatively, the induced velocity at the bridge, for example, can be monitored as the instrument is struck by a hammer at a large number of points across the surface [40]. Both types of measurements enable the modal wavefunctions and positions of line nodes to be mapped across the surface of the shell.

The two modes illustrated in fig. 10(b) both involve large rocking motions of the bridge. They are therefore strongly coupled to the bowed string, leading to a potential wolf-note problem, should the coupling be too strong (section 2.4). They give rise to the characteristic double peak usually observed in the measured input admittance at the bridge (induced velocity per unit force).

In fig. 10, the lower frequency mode at 423 Hz involves similar motions of the top and back plates, with only a small change in net volume. The mode involves a shearing motion of the top plate relative to the back and associated tipping of the side ribs. This results in a more nearly hinged boundary condition on the plate edges. The modal frequencies will therefore be intermediate between those of the rigidly and freely supported plates. In contrast, the higher frequency mode at 480 Hz involves large amplitude motions in opposite directions in the front and back plates. There is therefore a volume changing *breathing mode* acting as a strong source of monopole radiation, whereas the lower frequency mode radiates much less strongly as a dipole source.

The relative sizes of the two peaks will therefore differ markedly when the response to a force at the bridge is measured at the bridge or in the radiation field. The same is also true for the Helmholtz air resonance, which introduces a small peak in admittance measurements at the bridge, since it is only relatively weakly coupled to the shell modes, whereas it is a prominent feature in the radiation field response. In practice, it is much easier to make reliable measurements of the input admittance at the bridge than measurements of the radiated sound. This is due to the increasingly directional properties of the radiated sound on increasing frequency (see Weinreich [45]), differences in the *near* and *far* radiation fields, and the influence of the room acoustic, unless measurements are made in an anechoic chamber.

Fig. 11. Guitar-shaped violins by Stradivarius and Chanot.

5 Trapezoidal violin model

5.1 Historical

As our final illustration of the value of simple FEA models to elucidate the acoustics of the violin, we follow Savart's example [2] and consider the vibrational modes of a trapezoidal-shaped instrument. In particular, we consider the influence of the soundpost position on modal frequencies and waveforms. The model demonstrates why the symmetry-breaking soundpost position has such a large effect on the coupling of the bowed strings to the radiating vibrational modes via the bridge.

Although the modern violin is essentially unchanged in geometric form from that of the earliest Cremonese instruments, the shape can be modified to quite a large extent while still sounding like a violin. In folk-cultures, the shell of the violin is sometimes replaced by a simple rectangular box – even a suitably stringed tea-kettle has been demonstrated in public lectures sounding somewhat like a violin! Stradivarius also experimented with the shape, notably in the design of a guitar-shaped violin (the Tom Taylor Strad 1732) shown in fig. 11(a). This fine sounding violin was played by the distinguished soloist Joshua Bell in his early recordings and for the film score of *The Red Violin*.

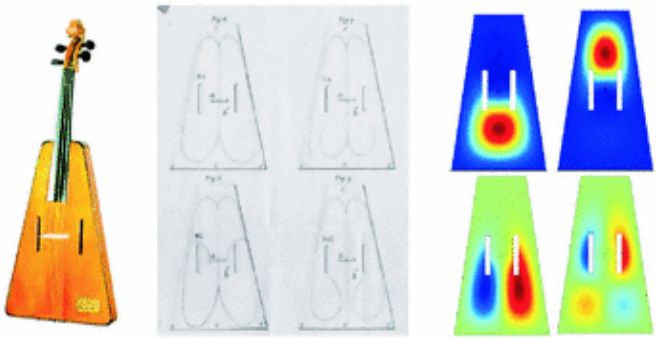

Fig. 12. (a) Savart violin 1823, (b) Chladni patterns using sand, and (c) finite element analysis of the lowest order modes of a trapezoidal plate with slots.

In the earlier part of the 19th century, the French violin maker Vuillaume served his apprenticeship with Chanot, making guitar-shaped violins with flat plates, fig. 11(b), aimed at the rapidly developing mass market for inexpensive instruments. In blind listening tests by French academicians and distinguished musicians, the sound of such a violin was considered the equal of fine Cremonese instruments!

Subsequently, Felix Savart collaborated with Vuillaume in a detailed investigation of the acoustics of the violin [2]. He adopted a very modern approach by investigating a highly simplified structure, using a trapezoidal-shaped instrument with flat plates (1819), shown in fig. 12(a), to elucidate the basic physics. However, instead of an offset soundpost, he used a solid arch extending from the side ribs and pressing centrally on the top plate.

Savart made extensive use of Chladni patterns to investigate the vibrational modes of individual violin plates (including those of valuable Cremonese instruments) and the trapezoidal violin, exciting the plates at the edges by a bow and using sand to form the nodal patterns. Examples of Chladni patterns for the trapezoidal violin are shown in fig. 12(b). All the illustrated modes are asymmetric, as expected from the construction of the violin with its centrally placed support rather than an offset soundpost. For comparison, fig. 12(c) illustrates the lowest-order symmetric and asymmetric modes computed for a slotted trapezoidal flat plate with fixed edges, but no additional soundpost constraint. The asymmetric modes are very similar to those expected from Savart's observations.

In blind-listening tests, the sound of the trapezoidal violin was also considered equal to that of Stradivari and Guarneri instruments. Such tests, although no more reliable than many such modern day comparisons, showed that the detailed shape of the violin cannot be particularly important in determining its tonal quality. This justifies our approach of using simple models to elucidate the essential physics.

5.2 A model calculation

In our example, we use the COMSOL FEA shell package to illustrate the vibrational modes of the shell of a trapezoidal violin, with slots to mimic the effect of the *f*-holes, but with a conventional offset soundpost between the plates rather than the arched structure used by Savart. The flat trapezoidal plates had length 30 cm, and widths of 20 cm and 10 cm at the bottom and top with ribs 3 cm high. All plates were of uniform density $\rho = 500\,\mathrm{kg\,m^{-3}}$, with front plate thicknesses 3 mm, back plate 4 mm and side walls 1 mm. For simplicity, the elastic constants were taken to be isotropic with $E = 10^{10}\,\mathrm{Pa}$ and damping terms equivalent to frequency independent Q-values for all modes of 50. The structure was supported by three orthogonal weak springs at the four corners of the lower plate.

The shell structure was excited by a sinusoidal force $Fe^{i\omega t}$ at the top of the bridge, to mimic the force from the partials of the bowed string. At low frequencies, the bridge can be considered as a rigid body, so that the "bowing" force can be reproduced by an equal force parallel to the top plate, with additional equal and opposite perpendicular forces exerted by the two bridge feet symmetrically placed across the central axis. The bowing force parallel to the top plate will tend to rotate the shell of the instrument about its longitudinal axis. As the rotational inertia of the instrument is large, such vibrations will be small and will decrease with increasing frequency. Acoustically, the most important forces are the perpendicular forces transmitted via the two feet of the bridge, which will excite the shell modes via the induced motion of the island region between the *f*-holes and the soundpost connecting to the back plate.

Figure 13 shows the calculated energy transfer per unit force at the bridge to the vibrational modes, as a function of frequency and position of the soundpost offset from the central axis by 0, 5, 10, and 15 mm. Peaks in the energy dissipation curves, plotted on a logarithmic scale, indicate the frequencies of the damped normal modes. Below the graph, the calculated modal patterns are shown for prominent peaks for the soundpost, first in a central position and then offset by 15 mm.

For a centrally placed soundpost, only asymmetric modes of the shell structure can be excited – as in Savart's measurements. In contrast, on offsetting the soundpost, both asymmetric and symmetric modes are excited, with an increase in energy transfer at the resonant frequency

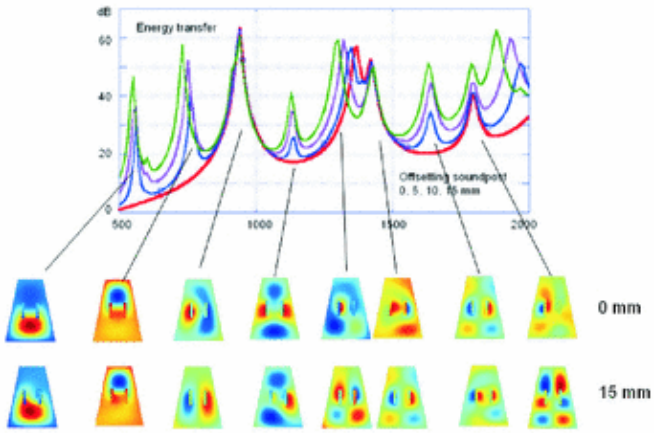

Fig. 13. Energy transfer for a trapezoidal violin with slots, excited by equal and opposite forces at feet of bridge, as a function of soundpost offset from central axis (0, 5, 10 and 15 mm), for a couple exerted by centrally placed bridge. The modal terns illustrate the effect of offsetting the soundpost by 15 mm from its central position.

of the lowest order symmetric modes approaching 60 dB. The increase in radiated sound at low frequencies would be even greater, since the symmetric modes are much more efficient sources of acoustic radiation.

It is also interesting to note the relatively small effect that the soundpost position has on the modal frequencies, despite the dramatic changes in coupling to the bridge. Above 1 kHz the amplitudes of both the symmetric and asymmetric modes are strongly dependent on soundpost position, with offsetting the soundpost increasing the energy transfer in some frequency ranges but decreasing it in others. Such calculations illustrate the very strong dependence of overall timbre of an instrument for large-scale changes in position of the soundpost. The same would almost certainly be true for conventionally shaped violins.

In practice, the skilled instrument maker and instrument restorer takes great care in adjusting the position of the soundpost, often to within a fraction of a mm, to optimise the tone quality of a valuable instrument. Such attention to the violin's *set-up* and associated tonal properties almost certainly contributes to the perceived superior sound of valuable Cremonese instruments over many modern instruments, which rarely have the advantage of such skillful optimisation.

6 Sound radiation and tonal quality

We now briefly consider the age-old problem of correlating the perceived tone quality of violins with their acoustic properties. As a physicist, one has to believe that some kind of correlation must exist. In contrast, many dealers, makers and players believe that the love and affection of a great player for a violin and the way it has been played in recent years are just as important in determining the quality of sound. In reality, it is almost certainly the way that the player's auditory responses and technique adjust to the acoustical properties of the violin, which accounts for the apparent improvement in tone with playing that is often perceived!

When the acoustic wavelength is larger than the dimensions of the body of the instrument – typically below about 1 kHz – the radiated sound can be considered as a superposition of point monopole, dipole and quadrupole sources, with radiation efficiencies varying with frequency as w^2, w^4, w^6 respectively (see Hill and Richardson [33] for a multi-pole analysis of guitar sounds). In this regime, most of the sound is therefore radiated isotropically by the monopole component, with the dipole and quadrupole components increasing in strength. Above a *cross-over*

frequency of around 1–2 kHz, the acoustic wavelength becomes shorter than the wavelength of the dispersive flexural waves in the plates, so that interference between the sound radiated from adjacent regions becomes important. The individual plates then act as baffled radiators, with the sound becoming increasingly directional (Weinreich [45]), and energy radiated proportional to the square of the velocity displacements integrated over the plate surfaces.

In formal terms, the sound pressure at a distance r and polar coordinates (θ, ϕ) for a sinusoidal force per unit sinusoidal force at the bridge at the bridge can be expressed as

$$p(r, \theta, \phi) = \sum_n \frac{R_n(r, \theta, \phi) c_n}{m_n(\omega_n^2 - \omega^2 - i\omega\omega_n/Q_n)} \tag{13}$$

where ω_n, m_n and Q_n are the frequencies, effective masses at the bridge and Q-values of the normal modes of the complete violin structure (including the bridge, fingerboard, neck, etc) and, strictly speaking, the coupled modes of the performance space into which the violin radiates. $R_n(r, \theta, \phi)$ represents the directionality and positional dependence of the radiated sound and c_n represents the coupling strength of the structural modes to the radiation field. $R_n(r, \theta, \phi)$ will vary markedly with both distance and frequency. The intensity of the sound experienced by the player will be dominated by direct sound from the violin, while the sound experienced by the listener will be strongly *coloured* by the acoustics of the performance space. This is almost certainly why a player finds it far easier to differentiate between the quality of different violins than the listener at a distance. The sounds they hear are very different, and the more resonant the acoustic, the larger such differences become. When played in a resonant acoustic, almost any violin played by a good player appears to have a fine sound - rather like one's own singing voice in a marble-walled bathroom.

Another way to consider the radiated sound is to consider the response in the time-domain. Applying a sharp tap or impulse to the bridge is equivalent to excitation by a wide-band frequency source. The resulting transient response is simply the Fourier transform of the spectral response – and vice versa. This will also be true for the sound heard by the listener in the performance space, which will include the additional reflections and reverberant decay from the surrounding reflecting walls, which can be significantly louder than the direct sound from the violin. Once the impulse response $p(t)$ is known for a particular position of the violin and listener in the performance space, the sound pressure $P(t)$ for an arbitrary force $f(t)$ at the point of string support on the bridge can be determined from the convolution of $f(t)$ with $p(t)$,

$$P(t) = \int_{-\infty}^{t} f(t')p(t - t')dt' \tag{14}$$

If the sound is monitored close to the violin, the impulse response will be dominated by the excited modes of the violin decaying with a typical exponential time constant ∼30–50 ms, though excited string modes ring for much longer. If the sound is monitored at a distance from the violin, the transient impulse response will include all the echoes and reverberation from the performance space. For a typical Sabine 60 dB decay-time of 2 seconds, the decay of the impulse response from the violin will be increased to well over 100 ms–increasing the apparent *ringing* quality of the violin, which is one of the attributes of the sound of a violin that appears to be correlated with its intrinsic quality. This is particularly true when the violin is played with vibrato (frequency modulation), due to the interference of the immediately received sound with delayed reflections at a different frequency, which leads to more complex and aurally more interesting waveforms [18, 49].

The inherent ringing quality of a violin will clearly be related to the damping and Q-values of the excited structural modes, which could be just as important as their specific frequencies in determining the quality of a violin. This is consistent with the way that violin makers generally choose wood with a strong ringing quality (low damping). However, the distinguished American violin maker, Joseph Curtin, has recently observed that, to the contrary, the plates of fine Italian violins often appear to be rather heavily damped [50]. This might also be because Cremonese plates often tend to be somewhat lighter than those of many modern makers, the damping being a function of both vibrating mass and the inherent losses. This is clearly an area for more research.

7 Summary

In this article we have emphasised the importance of the spatial distribution of the modal wavefunctions in determining the coupling of the string vibrations to the body of the instrument and ultimately to the radiated sound. We have highlighted the continuing role of Chladni pattern measurements as an aid to understanding the physics of the violin and to makers in optimising the acoustical properties of the plates during the carving stage. Modern techniques like laser interference holography, finite element analysis and modal analysis provide rather more information about the wave functions than Chladni measurements. This has been demonstrated by illustrative FEA calculations on model guitar- and trapezoidal-shaped plates, which enable us to assess the relative contribution to the overall acoustical properties of the bridge, *f*-holes, soundpost, bass bar, arching and anisotropy. A finite element analysis of the shell modes of a trapezoidal shaped violin demonstrates the importance of the offset soundpost in exciting both symmetric and asymmetric modes of the shell, which has a dramatic effect on the radiated sound. We have concluded with a brief introduction to the problem of reliable assessment of violin quality and have highlighted the influence of the room acoustics, in addition to the inherent damping properties of the violin, resulting in the difference in sound of a violin heard by the player and the listener.

References

1. F.A. Saunders, J. Acoust. Soc. Am. **25**, 491 (1953)
2. F. Savart, Mémoire sur la construction des Instruments à cordes et à archet (Deterville, Paris 1819): see also translations of selected works in ref. [3]
3. C.M. Hutchins, Musical Acoustics, Part I (Violin Family Components) and II (Violin Family Functions) edited by Hutchins, Benchmark papers in Acoustics, Nos. 5 and 6 (Dowden, Hutchinson and Ross, Stroudsburg, Pennsylvania 1975, 1976)
4. C.M. Huthchins, V. Benade, *Research Papers in Violin Acoustics 1975–1993,* Vols. 1 and 2 (Acoustical Society of America, New York, 1997)
5. C.M. Hutchins, J. Acoust. Soc. Am. **75**, 1421 (1983)
6. C.M. Hutchins, The Scientific American (1981, October), p. 171
7. L. Cremer, *The Physics of the Violin* (MIT Press, Havard, 1984)
8. N.H. Fletcher, T.D. Rossing, *The Physics of Musical Instruments* 2nd edn. (Springer-Verlag, New York, 1998)
9. M.E. McIntyre, J. Woodhouse, Acustica **43**, 93 (1979)
10. R.T. Schumacher, J. Acoust. Soc. Am. **43**, 109 (1979)
11. M.E. McIntyre, R.T. Schumacher, J. Woodhouse, Acustica **49**, 13 (1981)
12. J. Woodhouse, P.M. Galluzzo, Acustica **90**, 579 (2004)
13. C.E. Gough, Acta Acustica **91**, 229 (2005)
14. C.G.B. Baker, C.M. Thair, C.E. Gough, Acustica **4**, 70 (1980)
15. C.E. Gough, Acustica **44**, 673 (1980)
16. J.C. Schelling, J. Acoust. Soc. Am. **35**, 326 (1963)
17. C.E. Gough, Acustica **49**, 124 (1981)
18. C.E. Gough, Acta Acustica **91**, 229 (2005)
19. C.M. Hutchins, The Acoustics of Violin Plates, Scientific American (October, 1981), p. 71
20. J.C. Schelling, J. Acoust. Soc. Am. **53**, 26 (1973)
21. J.C. Schelling, Catgut Acoust. Soc. Newsletter (1971) No. 16 11; reprinted in ref. [3, Vol. 1 328–333]
22. C.V. Raman, Indian Assoc. Cultivation Sci. Bull. **15**, 1 (1918); reprinted in [Part 1 149–180][3]
23. J.H. Smith, J. Woodhouse, J. Mech. Phys. Solids **48**, 1633 (2000)
24. M. Hacklinger, Acustica **39**, 324 (1978)
25. J. Woodhouse, Acustica **91**, 155 (2005)
26. E.V. Jansson, Acustica **83**, 337 (1997)
27. E.V. Jansson, Catgut Acoust. Soc. Newsletter **19**, 13 (1973); reprinted in [3, Part 2 145–154]
28. M. Heckl, Acustica **10**, 109 (1960)
29. E. Reissner, Q. Appl. Math. **13**, 279 (1955)
30. G.W. Roberts, Ph.D. thesis (Cardiff University 1986); reprinted in part in [4, Part 1, 575]

31. G.A. Knott, MSc Thesis (1987), Naval Postgraduate School, Monterey, Ca; Reproduced in [4, Vol. 1 508]
32. G. Bissinger, Acustica **90**, 590 (2004)
33. T.J.W. Hill, B.E. Richardson, S.J. Richardson, SMAC 03 (Royal Swedish Academy of Music, Stockholm, 2003), p. 129
34. B.E. Richardson, G.W. Roberts, SMAC 83 (Royal Swedish Academy of Music, Stockholm, 1985), p. 285
35. L. Cremer, J. Acoust. Soc. Am. **48**, 988 (1970)
36. N.E. Molin, L.-E. Lindgren, E.V. Jansson, J. Acoust. Soc. A. **83**, 281 (1988)
37. O.E. Rogers, Catgut Acoust. Soc. J. **1**, 29 (1990); reprinted in [4] [Vol. 1], pp. 475–479
38. info@comsol.com
39. E.A. Emmerling, R.A. Kloss, Forsch. Ing.-Wes. **45**, 6 (1979): see Fig. 11.4 in [7]
40. F.D. Marshall, J. Acoust. Soc. Am. **77**, 695 (1985)
41. N.-K. Molin, A.O. Wahlin, E.V. Jansson, J. Acoust. Soc. Am. **90**, 2192 (1991)
42. L. Burckle, H. Grissino-Mayer, Dendrochronologia **21**, 41 (2003)
43. J. Woodhouse, Acustica **91**, 155 (2005)
44. data kindly supplied by Bissinger
45. G. Weinreich, J. Acoust. Soc. Am. **101**, 2338 (1997)
46. H.C. Bennet-Clark, D. Young, J. Exp. Biol. **173**, 123 (1992)
47. F. Savart, Cours de Physique Experimentale, professeur au Collège de France pendant l'année scolaire 1838–1839, L'Institut **8** (1840), Transl. by Donald Fletcher
48. H.-J. Stöckmann, Eur. Phys. J. Special Topics **145**, 15 (2007)
49. J. Meyer, Acustica **76**, 283 (1992)
50. J. Curtin, Proc. Int. Symp. Musical Acoustics, CSA-CAS 11 (1998)